Corrosion analysis of renewable inhibitor *Citrus aurantifolia* peels extract for API 5L Grade B steel in acid solution

A. Pradityana,[1]* F. Khosfirah,[1] P.I. Santosa[2] and W.B. Wan Nik[3]

[1]Department of Mechanical Industrial Engineering, Vocational Faculty, Institut Teknologi Sepuluh Nopember Surabaya, 60111, East Java, Indonesia
[2]Department of Shipping Engineering, Faculty of Engineering, Universitas Muhammadiyah Surabaya, 60113, East Java, Indonesia
[3]Faculty of Ocean Engineering Technology and Informatics, Universiti Malaysia Terengganu, 21030 Kuala Nerus, Terengganu, Malaysia
**E-mail: atriapradityana@gmail.com*

Abstract

An extract from the peels of *Citrus aurantifolia* (CA) has been investigated as a corrosion inhibitor on API 5L grade B material in acid solution. It was confirmed by FT-IR measurements that the CA peels contained functional groups that could favor corrosion inhibition. The effectiveness of corrosion inhibition was examined through the use of electrochemical techniques and scanning electron microscopy. In 1 M H_2SO_4, the effectiveness of the inhibitor (200 mg/L) was 99.2% (from PDP measurements) or 99.1% (from EIS measurement). The Langmuir isotherm model was used to examine the adsorption behavior of the extract. The negative and low Gibbs free energy values supported that the inhibitor was adsorbed on the surface of API 5L Grade B material. This value can also be used as a reference that CA peels extract has a physisorption ability. SEM images show that the surface of the specimen in the presence of the inhibitor forms a thin layer that is thought to be able to inhibit the corrosion rate, whereas on the surface of the specimen in the absence of inhibitor, no thin layer is formed. The results show that under acid corrosion, CA peels extract effectively inhibits the corrosion of API 5L Grade B material because it forms a thin film on the surface of the material.

Received: November 13, 2023. Published: February 25, 2024 doi: 10.17675/2305-6894-2024-13-1-20

Keywords: *Citrus aurantifolia peels, H_2SO_4, Langmuir isotherm, electrochemical polarization.*

1. Introduction

The reaction of metals with their environments is called corrosion and is irreversible. There are many methods that can be employed to control the corrosion process. One of the efforts that can be used to control corrosion of metals due to environmental impacts is by adding corrosion protection compounds, also known as inhibitors [1–4]. Corrosion inhibitors decrease the corrosion rate by forming a passive layer in the form of a thin film on the surface of the material that serves as a barrier between the metal and the corrosive medium. An acid environment can be a major cause of corrosion. In fact, acid environments are commonly

used in extraction and refining operations, pickling, chemical industry, infrastructure and civil engineering [5–11].

As sulfuric acid is a strong acid employed in a variety of chemical methods, it is one of the most commonly utilized pickling agents. In the steel manufacturing process, sulfuric acid is mainly used for cleaning rust and film from billets and rolled sheets and to clean out contamination from petroleum refineries, including gasoline [6, 10].

Chromate and imidazole are examples of chemical corrosion inhibitors. Both have adverse characteristics, including non-biodegradable, expensive, dangerous, harmful, and toxic. In the 20th century, the scope of corrosion inhibitors began to undergo gradual changes [7, 12–15]. The use of natural plant extracts as corrosion inhibitors started to develop. Knowing the characteristics of chemical corrosion inhibitors is one of the reasons for the development of corrosion inhibitors obtained from natural plant extracts. The advantages of using a corrosion inhibitor made from natural plant extracts include the abundant availability in nature, low cost, low or non-existent toxicity, high efficiency, and renewability [1, 2, 4, 16–19].

There are a number of reasons why a natural plant extract can be used as an inhibitor, in particular, because they contain amino acids, aromatics, alkaloids, and tannins [14, 17]. In addition, the presence of unshared electrons, covalent double bonds with P, O, N, S and heteroatoms also have a beneficial role in inhibiting corrosion. Many studies show that some parts of natural plants contain such ingredients, including leaves, seeds, roots, flowers, and fruit skins [6, 16, 21–23].

Many studies have used plant extracts as inhibitors, one of which is the research of N. Al-Akhras and Y. Mashaqbeh [6]. They used *Eucalyptus* leaf extract as a corrosion inhibitor for steel building foundations. Corrosion inhibitors made from natural materials have advantages compared to those made from chemicals such as biodegradability, non-toxicity, ecological friendliness, low cost, abundant availability, renewability, and safety in use [24]. The results obtained were positive, including a decrease in the corrosion rate of steel treated with eucalyptus leaf extract compared to untreated steel, a decrease in the amount of rust in steel with an increase in the concentration of inhibitor of *Eucalyptus* leaf extract, and an increase in the flexural performance of corroded steel when compared to that not treated with inhibitors [6].

In another study by R. Haldhar *et al*. [12], *Citrus aurantifolia* (lime) leaf extract was used on mild steel at a sulfuric acid concentration of 0.5 M. Mild steel was treated with inhibitors at concentrations varying from 0 to 250 mmol/L. It showed improved results in the form of increasing the efficiency of corrosion prevention by >93% at an inhibitor concentration of 250 mg/L. Amino acids are among the inhibitors that are environmentally friendly, non-toxic, biodegradable, inexpensive, and easily soluble in liquid media. Amino acids have 10 types of chemical classification and 20 types of structures [25]. The efficiency level of amino acids as inhibitors depends on the level of absorption in the targeted material [26]. Therefore, amino acids have their own advantages in each type of structure for each material to be treated with amino acids as inhibitors. According to M. Yeganeh *et al*. [17],

methionine is one of the amino acids used for inhibition of 309S stainless steel in 1 M sulfuric acid solution. EIS results showed an increase in corrosion resistance from 54 to 1750 $\Omega \cdot cm^2$ and an increase in inhibition efficiency reaching a maximum of 97%. This occurs as the concentration of L-methionine increases from 0 to 700 ppm.

Citrus aurantifolia (CA) is very popular for its unique taste and attractive color. This fruit has a variety of ingredients, including vitamin C, flavonoid compounds, limonoids, phenolic acids, alkaloids, phytosterols, aglycones, glucosides, nomilin, limonins and other biologically active compounds [12]. Flavonoids and tannins are antioxidant compounds. CA peels contain flavonoid compounds with a higher concentration than other parts that can be used as antioxidants. In previous research, CA leaves extract had been used to inhibit corrosion of carbon steel in 1 M HCl solution. The test was carried out with a variety of concentrations and resulted in the best inhibition efficiency reaching 97.51% at 2.5% inhibitor concentration.

The most common types of flavonoids found in CA extracts are apigenin, routine, quercetin, kaempferol and nobiletin. The *n*-hexane fraction of both CA fruit peels and leaves showed good acetylcholinesterase inhibitory activity with IC (50) values in the range 91.4–107.4 mg mL^{-1} [21]. These flavonoid compounds are antioxidants because they can inhibit free radical attack, so they are thought to help inhibit corrosion.

In this research, we used CA peels extract which is a renewable corrosion inhibitor for API 5L Grade B steel in H_2SO_4 1 M solution. As previously explained, the CA peels extract contains ingredients that have an important role in inhibiting corrosion. In this study, various concentrations of CA peels extract were used, including 50, 100, 150, 200, and 250 mg/L. The inhibition was studied using electrochemical measurements. The chemical structure of the extract was studied using FT-IR spectroscopy and the adsorption mechanism was studied using SEM.

2. Materials and Methods

2.1. CA peels extraction

The CA peels that obtained was the leftover from selling chicken soup in the ITS campus area. Then CA peels were cleaned and dried in the sun for a few days so that the peels were completely dry. After drying under the sun for 3×24 hours, they were oven-dried at a temperature of 40°C for 4 hours. This was done so that the CA peels did not contain water anymore. The dried skin was made into powder using a crushing machine. After the powder was produced, CA peels were macerated with methanol for 3×24 hours. The next step was to remove the remaining methanol in a rotary evaporator and the CA peels extract was then ready to use.

2.2. Materials

The material used was an API 5L (ASTM A53) grade B steel specimen with dimensions of 10×10×16 mm. It was used for polarization and impedance testing. According to the ASTM

G102 standard, specimens with dimensions of 30×30×6 mm are used for weight reduction measurements. The chemical composition of API 5L Grade B steel is C 0.21%; Mn 0.45%; P 0.013%; S 0.01%; Si 0.23%.

2.3. Corrosion medium preparation

1 M H_2SO_4 solution was used as the corrosive medium.

2.4. Electrochemical measurements

Electrochemical measurements included potentiodynamic polarization (PDP) and Electrochemical Impedance Spectroscopy (EIS). Both PDP and EIS measurements were carried out using the Autolab Potentiostat Galvanostat PGSTAT302N AUT84992. PDP measurements were supported by Nova 1.8 software, while EIS measurements were supported by Zview software. For PDP measurement, a platinum (Pt) counter electrode was used while the reference electrode was Ag/AgCl. The start potential was –0.100 V and the end potential was +0.100 V. The area of the exposed material was 1 cm^2. The scan rate was 10 mV/s. For EIS measurements, the AC signal amplitude was 10 mV.

2.5. FT-IR spectroscopy measurements

This analysis was conducted to determine the functional groups contained in the inhibitor extract. From the FTIR results on corrosion inhibitors, various bonds are shown in the form of peaks. This measurement was carried out at room temperature.

2.6. Corrosion morphology analysis

This measurement was carried out after getting the best inhibition efficiency in the measurement of weight loss. In this case, addition of 200 mg/L inhibitor and an immersion time of 3 hours were used. The scanning electron microscopy (SEM) test aims to determine the morphological differences between the surface of API 5L grade B steel specimens that were protected by CA peel extract inhibitor and those that were not protected. Phenom Pro-X type SEM equipment was used. This tool has an optical electron magnification capability of 20–130,000 times and can be zoomed up to 12x, with a resolution of more than 14 nm, optical magnification capability of 20–135 times, as well as imaging and analysis at 5 kV, 10 kV and 15 kV power.

3. Results and Discussion

3.1. CA peels extract characterization

The FTIR measurement outcomes of the extract from CA peels are shown in Figure 1. Five peaks are created, where each peak (wavelength) corresponds to multiple functional groups. Amine and amide compounds with N–H functional groups form a peak at 3353.98 cm^{-1}, alkane compounds with C–H functional groups form a peak at 2922.09 cm^{-1}, while

aldehyde, ketone, carboxylic acid, and ester molecules with C=O functional groups form a peak at 1716.70 cm^{-1}.

Alcohols, ethers, carboxylic acids, and ester molecules with C–O functional groups are present as a peak at 1197.54 cm^{-1}. Alkyl halide, ether, and ester compounds with C–F and C–O functional groups form a peak at 1042.41 cm^{-1}. Some functional groups among these groups indicate the presence of flavonoid chemicals in CA fruit peel extract. The flavonoid functional groups include C–H, C=O and C–O.

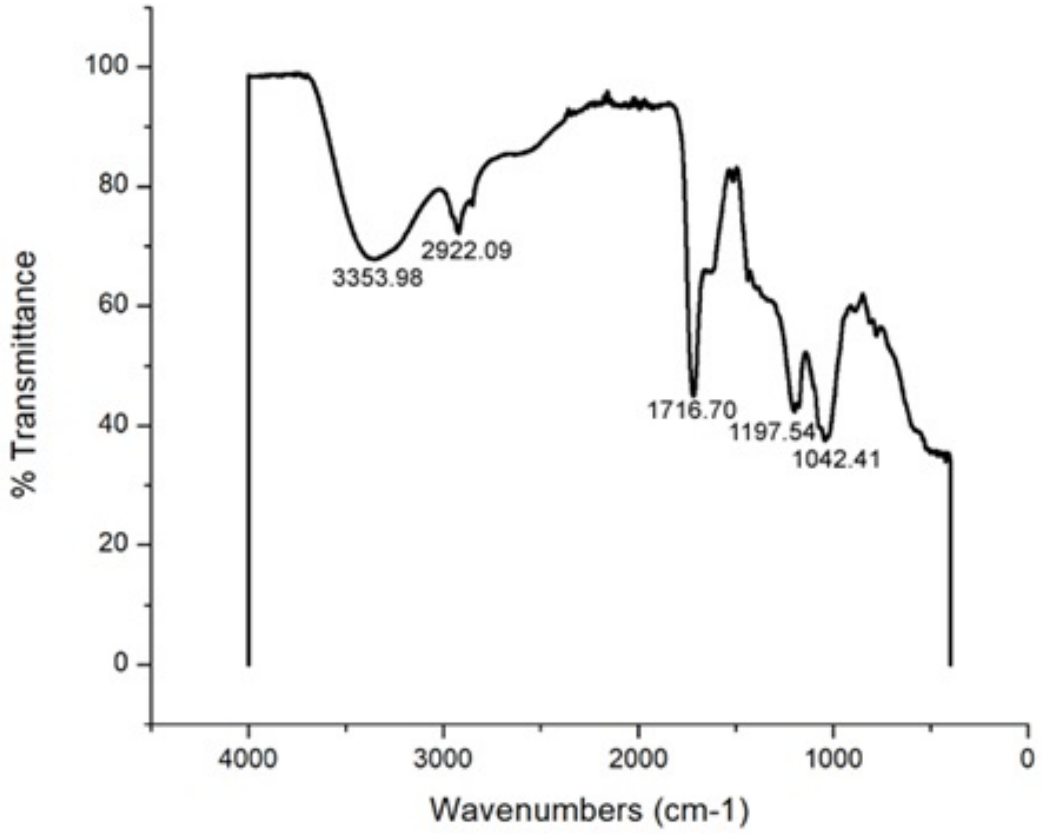

Figure 1. The result of FTIR measurement on CA peels extract.

3.2. Potentiodynamic polarization (PDP) curves

The Tafel curves for API 5L Grade B steel in 1 M H_2SO_4 solution in the absence and in the presence of the CA peels extract are presented in Figure 1. The parameters based on the polarization measurements are shown in Table 1. The inhibition efficiency can be calculated by the expression:

$$\%IE = \frac{\left(i_{\text{without inhibitor}} - i_{\text{with inhibitor}}\right)}{i_{\text{without inhibitor}}} \cdot 100\%$$

where i is the corrosion current density of API 5L Grade B steel [27].

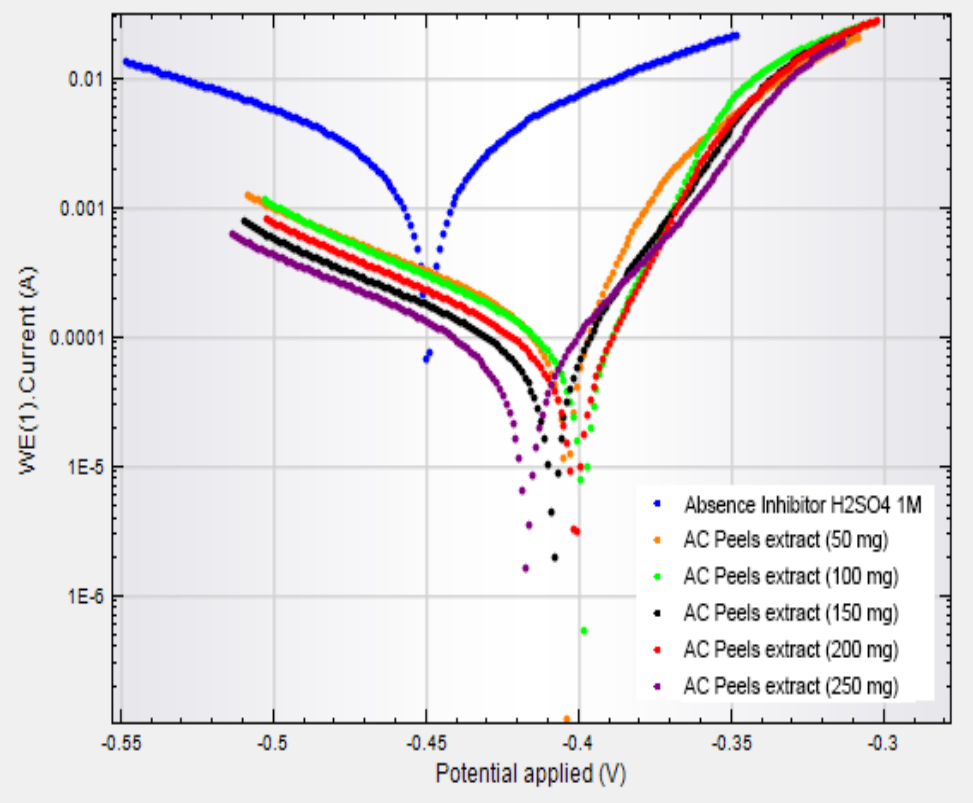

Figure 2. Effect of the CA peels extract concentration on Tafel curves for API 5L Grade B steel in 1 M H_2SO_4 solution.

From the PDP measurement, polarization data is generated which is used to analyze the adsorption mechanism. Extrapolation results from the polarization curve gave the values of i_{corr} and E_{corr} [2], [4], [12]. These values are used to calculate the corrosion rate. Figure 1 shows the Tafel curves for various inhibitor concentrations in 1 M H_2SO_4 solution [28]. The results of the extrapolated Tafel plots are shown in Table 1.

Table 1. Effect of the CA peels extract concentration on polarization parameters for API 5L Grade B steel in 1 M H_2SO_4 solution.

Inhibitor concentration	***E*corr (mV)**	***i*corr (μA/cm²)**	***CR* (mm/year)**	***IE* (%)**
None	–436	6456	75.0	–
50	–403	101	1.18	98.4
100	–397	81.5	0.947	98.7
150	–407	67.4	0.784	98.9
200	–400	49.2	0.571	99.2
250	–418	72.0	0.837	98.8

The optimum inhibition efficiency value of 99.2% was obtained upon the addition of 200 mg/L CA peels extract (Table 1). This result indicates that the corrosion rate of API 5L Grade B material can be inhibited effectively by increasing the concentration to 200 mg/L. The increase in inhibition efficiency value is proportional to the decrease in current density. The results of the PDP measurement were used to analyze the adsorption mechanism. Upon addition of 200 mg/L CA peels extract, the adsorption of inhibitor molecules to create a uniform layer on the metal surface resulted in a decrease in current density. The optimum inhibition efficiency was obtained at the addition of 200 mg/L inhibitor and decreased with an increase in concentration to 250 mg/L, presumably due to the physical adsorption mechanism. When the inhibitor concentration is above 200 mg/L (optimal concentration), the solution becomes saturated. There is also the possibility of a strong interaction between the inhibitor attached to the metal surface and the inhibitor molecules in the solution [3], [29]. This might cause the coating formed from the inhibitor to be released into the solution.

3.3. Electrochemical impedance spectroscopy plots

Constant phase element (CPE), solution resistance (R_s), and charge transfer resistance (R_{ct}) are parameters obtained from EIS measurements. Figure 3 shows the Nyquist plot for API 5 Grade B material in 1 M H_2SO_4 solution at various inhibitor concentrations. R_{ct} reflects the interaction that occurs between the metal surface and the solution which causes charge transfer between the two. The characteristics of the roughness and inhomogeneity of the electrode surface are indicated by the semicircular shape of the Nyquist plot (Figure 3) [3]. In addition, the time constant, which is related to CPE and R_{ct}, corresponds to the semicircle at the top of the frequency region. The general instance of the frequency response of an interface characterized by charge transfer and diffusion processes is illustrated by the equivalent circuit model (Figure 3). R_{ct} and other resistances including diffusion layer resistance, species buildup at the metal solution or interface, and inhibitor film resistance make up the polarization resistance at common frequencies. A variety of physical phenomena are displayed by CPE, including inhibitor adsorption, layer development, and surface inhomogeneity of roughness [3].

The charge transfer resistance (R_{ct}) values determine the frequency responses of these equivalent circuit models. The corresponding circuit model, which fits the EIS measurement result with a representative fitting example of Nyquist diagrams for material API 5L Grade B in 1 M H_2SO_4 solution, is illustrated in Figure 3. Table 2 presents the impedance parameters obtained from the fitting of the EIS data obtained experimentally to the equivalent circuit.

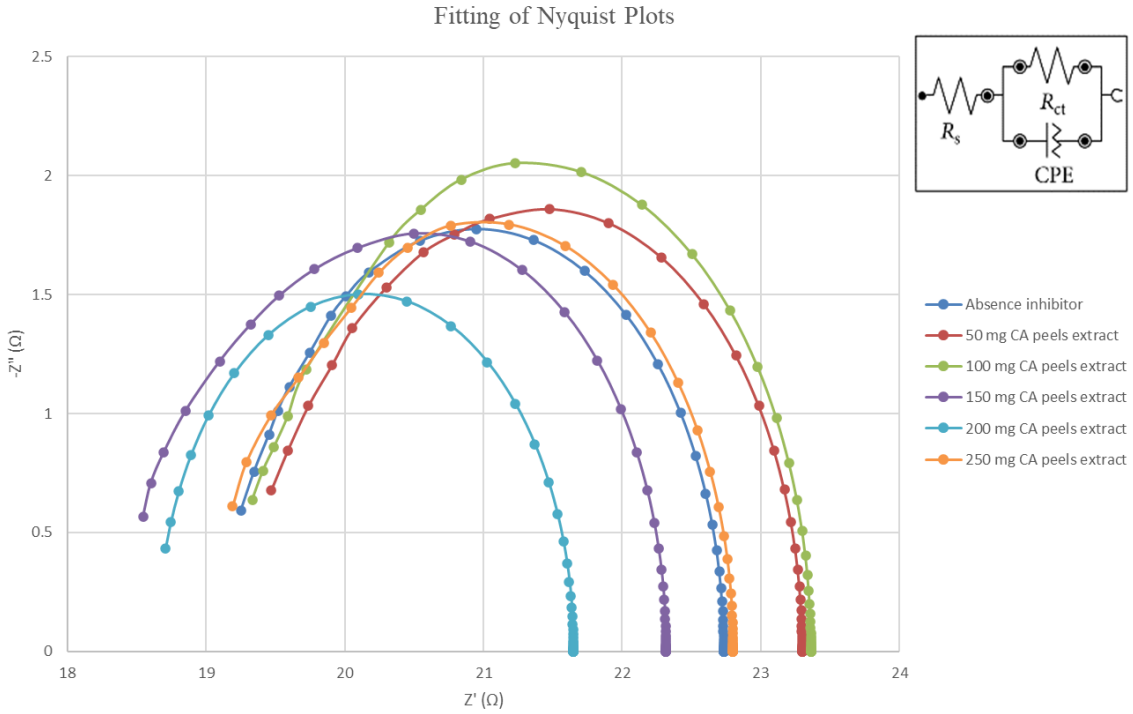

Figure 3. Effect of the CA peels extract concentration on Nyquist plots for API 5L Grade B steel in 1 M H_2SO_4 solution.

Table 2. Effect of the CA peels extract concentration on the electrochemical parameters for API 5L Grade B steel in 1 M H_2SO_4 solution.

Inhibitor concentration (mg/L)	***CPE* (μF)**	**R_{ct} (Ω)**	**R_s (Ω)**	***IE* (%)**
None	65.9	4.21	23.3	–
50	59.5	329	185	98.7
100	46.3	349	193	98.8
150	42.5	367	1.24	98.9
200	37.2	443	1.68	99.1
250	32.3	404	53.3	98.9

The level of inhibition caused by the presence of CA peels extract is shown by the R_{ct} value. The capacitive circle's diameter (Figure 3) obtained at an inhibitor concentration of 200 mg/L had the greatest diameter; the diameter in the absence of the inhibitor was smaller, showing that the CA peels extract inhibited the corrosion of material API 5L Grade B in 1 M H_2SO_4 solution and raised the charge transfer resistance [30]. Because of the formation of the oxide layer, increasing the R_{ct} value with an inhibitor addition of 200 mg/L generated an increased ability to hinder corrosion [31]. This method's 99.1% inhibitory efficiency (*IE*%) (Table 2) is in good accord with the potentiodynamic polarization method.

3.4. Adsorption isotherm and calculation of thermodynamic parameters

Corrosion inhibitors may interact with the material surface by isothermal adsorption. The linear curve plot of the isothermal adsorption equations describes the corrosion inhibitor's adsorption pattern. There are several kinds of adsorption mechanisms [32]. The approach that performed best in this research is the Langmuir adsorption. The Langmuir equation used is as follows:

$$K_{\text{ads}} = \frac{\theta}{(1-\theta)C_{\text{inh}}}$$

The constant that controls the adsorption-desorption is known as K_{ads}, the inhibitor concentration is denoted C_{inh}, and the surface coverage fraction is denoted θ.

The mechanism of CA peels extract reduction on material API 5L Grade B surface can be analyzed using the thermodynamic parameters, including the variations in the adsorption free energy (ΔG^0_{ads}), enthalpy (ΔH^0_{ads}), and entropy (ΔS^0_{ads}). The following is the equation for the changes in free energy of adsorption [33]:

$$\Delta G^0_{\text{ads}} = -RT\ln(K_{\text{ads}}A)$$

where T is the absolute temperature (K), A is the molar concentration of water in the acid solution, and R is the gas constant (equal to 8.314 J K^{-1} mol^{-1}). The molar concentration of water is 55.5.

If the value of ΔG^0_{ads} is in the range from 0 to –20 kJ mol^{-1}, it suggests physisorption. In contrast, ΔG^0_{ads} values below –40 kJ mol^{-1} can indicate chemisorption [34]. Exothermic adsorption can be identified using the negative value of enthalpy ΔH^0_{ads}. The absolute magnitude of ΔH^0_{ads} for physisorption is less than that of chemisorption. The Van't Hoff equation was used to estimate ΔH^0_{ads}.

$$\ln K_{\text{ads}} = \frac{-\Delta H^0_{\text{ads}}}{RT}$$

The enthalpy of adsorption is ΔH^0_{ads}, and the absolute temperature is T. Adsorption process identification can be done with ΔS^0_{ads}. An excess of adsorption is indicated if the value of ΔS^0_{ads} is greater than zero. The formula was used to determine its value:

$$\Delta G^0_{\text{ads}} = \Delta H^0_{\text{ads}} - T\Delta S^0_{\text{ads}}$$

In this research, the ΔG^0_{ads} value (Table 3) is typical of physisorption. The spontaneity of CA peels extract adsorption on the material API 5L Grade B surface is ensured by the negative values of ΔG^0_{ads}. This result is consistent with what is said in Section 3.1 and supports the idea that CA peels extract adsorption is physisorption.

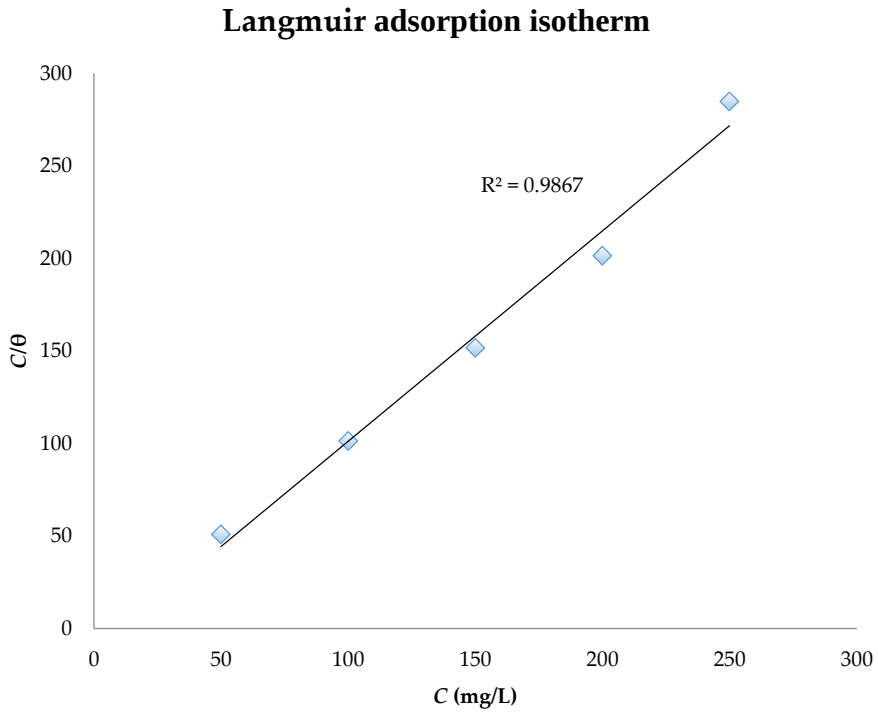

Figure 4. Langmuir isotherm for adsorption of CA peels extract on material surface.

Table 3. Thermodynamic parameters for API 5L Grade B material in 1 M H_2SO_4 solution.

Inhibitor concentration (mg/L)	ΔG^0_{ads} (kJ/mol)	ΔH^0_{ads} (kJ/mol)	ΔS^0_{ads} (J/mol·K)
50	–12.1	–8.06	13.3
100	–11.6	–7.58	13.3
150	–11.4	–7.37	13.3
200	–11.4	–7.40	13.3
250	–8.29	–4.28	13.3

3.5. Corrosion morphology

To provide concrete evidence, SEM analysis was conducted. Figure 5 illustrates the effect of the inhibitor on the microstructure of the top surface of the API 5 Grade B material. Figure 5(a) shows the surface of the material in the absence of inhibitor. The surface of the API 5 Grade B material shows some cracks after being corroded in acidic solution without inhibitor. In contrast, Figure 5(b) shows the formation of a thin layer on the surface of the material treated with CA peels extract inhibitor. Less damage is visible when the inhibitor is present. This demonstrates how successful the inhibitor is at preventing corrosion [22, 34, 35].

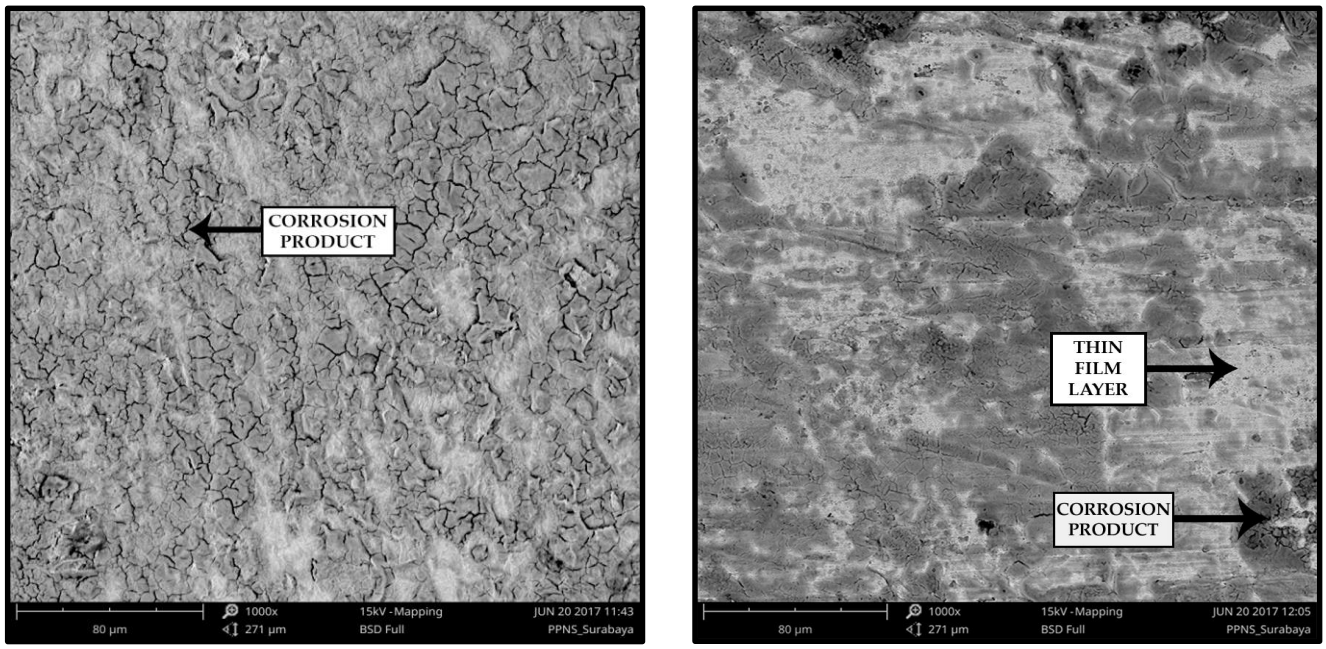

(a) (b)

Figure 5. Scanning Electron Microscope (SEM) images of API 5L Grade B material's surface (a) in the absence of an inhibitor and (b) in the presence of 200 mg/L inhibitor.

Conclusions

The addition of AC peels extract inhibitor is proven to reduce the corrosion rate of API 5L grade B steel material in the acid environment. The best result in this research was achieved using 200 mg/mL of the inhibitor. At this concentration, the PDP measurement gave the lowest i_{corr} value and the highest inhibitor efficiency of 99.2%. In addition, the EIS test also gave the best inhibition efficiency, namely 99.1%. This inhibitor efficiency is supported by the SEM study which shows that the surface of the material in the presence of the inhibitor shows a passive layer that functions as a surface protector of the material from corrosion.

Acknowledgments

The authors are grateful to Institut Teknologi Sepuluh Nopember Surabaya-Indonesia for facilitating the laboratories necessary for this research.

References

1. O.K. Abiola and A.O. James, The effects of *Aloe vera* extract on corrosion and kinetics of corrosion process of zinc in HCl solution, *Corros. Sci.*, 2010, **52**, no. 2, 661–664. doi: 10.1016/j.corsci.2009.10.026
2. G. Nugroho, A. Pradityana, N. Husodo, M. Mursid, G.D. Winarto and F.T. Putrandi, Mechanism of papaya leaf as organic inhibitor in corrosion process, *AIP Conf. Proc.*, 2018, 050017. doi: 10.1063/1.5046290

3. A.M. Fekry and M.A. Ameer, Electrochemical investigation on the corrosion and hydrogen evolution rate of mild steel in sulphuric acid solution, *Int. J. Hydrogen Energy*, 2011, **36**, no. 17, 11207–11215. doi: 10.1016/j.ijhydene.2011.05.149
4. A. Pradityana, Sulistijono, Winarto, E. Widiyono, B. Luwar and M. Mursid, Effect of temperature on the application of *Myrmecodia Pendans* extract for environmentally friendly corrosion inhibitor, *AIP Conf. Proc*., 2017, 030001. doi: 10.1063/1.4982261
5. B. Lin, J. Shao, Y. Xu, Y. Lai and Z. Zhao, Adsorption and corrosion of renewable inhibitor of *Pomelo* peel extract for mild steel in phosphoric acid solution, *Arabian J. Chem*., 2021, **14**, no. 5, 103114. doi: 10.1016/j.arabjc.2021.103114
6. N. Al-Akhras and Y. Mashaqbeh, Potential use of eucalyptus leaves as green corrosion inhibitor of steel reinforcement, *J. Build. Eng*., 2021, **35**, 101848. doi: 10.1016/j.jobe.2020.101848
7. T. Han, J.-X. Guo, Q. Zhao, T. Shen and S.-L. Zhang, Insights into the multiple applications of modified polyacrylamide as oilfield corrosion inhibitor and water phase tackifier, *Pet. Sci*., 2022, **19**, no. 1, 397–408. doi: 10.1016/j.petsci.2022.01.003
8. P.B. Matad, P.B. Mokshanatha, N. Hebbar, V.T. Venkatesha and H.C. Tandon, Ketosulfone Drug as a Green Corrosion Inhibitor for Mild Steel in Acidic Medium, *Ind. Eng. Chem. Res*., 2014, **53**, no. 20, 8436–8444. doi: 10.1021/ie500232g
9. F. Zulkifli, N. Ali, M. Sukeri, M. Yusof, Wan M. Khairul, R. Rahamathullah, M.I.N. Isa and W.B.Wan Nik, The Effect of Concentration of *Lawsonia inermis* as a Corrosion Inhibitor for Aluminum Alloy in Seawater, *Adv. Phys. Chem*., 2017, 8521623, 1–12. doi: 10.1155/2017/8521623
10. N. Ismail, S.M. Mujad, M.F.R. Zulkifli, V.O. Izionworu, M.J. Ghazali and W.B. Wan Nik, A review on application of marine algae as green corrosion inhibitors in acid medium, *Vietnam J. Chem*., 2022, **60**, no. 4, 409–416, 2022. doi: 10.1002/vjch.202200001
11. W.B. Wan Nik, O. Sulaiman, S.G. Eng Giap and R. Rosliza, Evaluation of Inhibitive Action of Sodium Benzoate on Corrosion Behaviour of AA6063 in Seawater, *Int. J. Technol*., 2014, 1, no. 1, 20–28. doi: 10.14716/ijtech.v1i1.39
12. R. Haldhar, D. Prasad and N. Bhardwaj, Extraction and experimental studies of *Citrus aurantifolia* as an economical and green corrosion inhibitor for mild steel in acidic media, *J. Adhes. Sci. Technol*., 2019, **33**, no. 11, 1169–1183. doi: 10.1080/01694243.2019.1585030
13. R. Dorothy, T. Sasilatha and S. Rajendran, Corrosion resistance of mild steel (hull plate) in sea water in the presence of a coating of an oil extract of plant materials, *Int. J. Corros. Scale Inhib*., 2021, **10**, no. 2, 676–699. doi: 10.17675/2305-6894-2021-10-2-13
14. B. El Ibrahimi, A. Jmiai, L. Bazzi and S. El Issami, Amino acids and their derivatives as corrosion inhibitors for metals and alloys, *Arabian J. Chem*., 2020, **13**, no. 1, 740–771. doi: 10.1016/j.arabjc.2017.07.013

15. A. Farhadian, A. Rahimi, N. Safaei, A. Shaabani, E. Sadeh, M. Abdouss and A. Alavi, Exploration of Sunflower Oil As a Renewable Biomass Source to Develop Scalable and Highly Effective Corrosion Inhibitors in a 15% HCl Medium at High Temperatures, *ACS Appl. Mater. Interfaces*, 2021, **13**, no. 2, 3119–3138. doi: 10.1021/acsami.0c18887
16. W.M.K.W.M. Ikhmal, M.F.M. Maria, W.A.W. Rafizah, W.N.W.M. Norsani and M.G.M. Sabri, Corrosion inhibition of mild steel in seawater through green approach using *Leucaena leucocephala* leaves extract, *Int. J. Corros. Scale Inhib*., 2019, **8**, no. 3, 628–643. doi: 10.17675/2305-6894-2019-8-3-12
17. M. Yeganeh, I. Khosravi-Bigdeli, M. Eskandari and S.R. Alavi Zaree, Corrosion Inhibition of l-Methionine Amino Acid as a Green Corrosion Inhibitor for Stainless Steel in the H_2SO_4 Solution, *J. Mater. Eng. Perform*., 2020, **29**, no. 6, 3983–3994. doi: 10.1007/s11665-020-04890-y
18. C. Zhu, H.X. Yang, Y.Z. Wang, D.Q. Zhang, Y. Chen and L.X. Gao, Synergistic effect between glutamic acid and rare earth cerium (III) as corrosion inhibitors on AA5052 aluminum alloy in neutral chloride medium, *Ionics*, 2019, **25**, no. 3, 1395–1406. doi: 10.1007/s11581-018-2605-4
19. A.A. Kruzhilin, D.S. Shevtsov, A.Yu. Potapov, Kh.S. Shikhaliev, O.A. Kozaderov, Ch. Prabhakar and V.E. Kasatkin, Novel inhibitory compositions based on 4,5,6,7-tetrahydro-[1,2,4]triazolo[1,5-a]pyrimidin-7-ol derivatives for steel acid corrosion protection, *Int. J. Corros. Scale Inhib*., 2022, **11**, no. 2, 774–795. doi: 10.17675/2305-6894-2022-11-2-22
20. A.A. Kruzhilin, D.S. Shevtsov, D.V. Lyapun, A.Yu. Potapov, Kh.S. Shikhaliev, O.A. Kozaderov, D.Yu. Vandyshev and V.B. Sulimov, 3-Alkylsulfonyl-5-amino-1,2,4-triazoles – new corrosion inhibitors of copper and copper-containing alloys, *Int. J. Corros. Scale Inhib*., 2022, **11**, no. 4, 1703–1715. doi: 10.17675/2305-6894-2022-11-4-19
21. M.R. Loizzo, R. Tundis, M. Bonesi, F. Menichini, D. De Luca, C. Colica and F. Menichini, Evaluation of *Citrus aurantifolia* peel and leaves extracts for their chemical composition, antioxidant and anti-cholinesterase activities, *J. Sci. Food Agric*., 2012, **92**, no. 15, 2960–2967. doi: 10.1002/jsfa.5708
22. B. Lin, J. Shao, Y. Xu, Y. Lai and Z. Zhao, Adsorption and corrosion of renewable inhibitor of *Pomelo* peel extract for mild steel in phosphoric acid solution, *Arabian J. Chem*., 2021, **14**, no. 5, 103114. doi: 10.1016/j.arabjc.2021.103114
23. A.M. Salim, N.M. Dawood and R. Ghazi, Pomegranate Peel Plant Extract as Potential Corrosion Inhibitor for Mild Carbon Steel in a 1 M HCl Solution, *IOP Conf. Ser.: Mater. Sci. Eng*., 2020, **987**, no. 1, 012019. doi: 10.1088/1757-899X/987/1/012019
24. A.M. Fekry and M.A. Ameer, Electrochemical investigation on the corrosion and hydrogen evolution rate of mild steel in sulphuric acid solution, *Int. J. Hydrogen Energy*, 2011, **36**, no. 17, 11207–11215. doi: 10.1016/j.ijhydene.2011.05.149

25. B. El Ibrahimi, A. Jmiai, L. Bazzi and S. El Issami, Amino acids and their derivatives as corrosion inhibitors for metals and alloys, *Arabian J. Chem*., 2020, **13**, no. 1, 740–771. doi: 10.1016/j.arabjc.2017.07.013
26. Wajilan, A. Fernandes and A. Wahyudianto, Effect of a mixture of paint and Rhizophora mucronata leaves extract as a natural inhibitor of marine steel in 3.5% NaCl solution, *Int. J. Corros. Scale Inhib*., 2021, **10**, no. 4, 1441–1453. doi: 10.17675/2305-6894-2021-10-4-5
27. A. Ostovari, S. Hoseinieh, M. Peikari, S. Shadizadeh and S. Hashemi, Corrosion inhibition of mild steel in 1 M HCl solution by henna extract: A comparative study of the inhibition by henna and its constituents (Lawsone, Gallic acid, α-d-Glucose and Tannic acid), *Corros. Sci*., 2009, **51**, no. 9, 1935–1949. doi: 10.1016/j.corsci.2009.05.024
28. R. Dorothy, T. Sasilatha and S. Rajendran, Corrosion resistance of mild steel (hull plate) in sea water in the presence of a coating of an oil extract of plant materials, *Int. J. Corros. Scale Inhib*., 2021, **10**, no. 2, 676–699. doi: 10.17675/2305-6894-2021-10-2-13
29. G. Serdaroğlu and S. Kaya, Organic and Inorganic Corrosion Inhibitors, *in Organic Corrosion Inhibitors*, Wiley, 2021, 59–73. doi: 10.1002/9781119794516.ch4
30. N. Al-Akhras and Y. Mashaqbeh, Potential use of *eucalyptus* leaves as green corrosion inhibitor of steel reinforcement, *J. Build. Eng*., 2021, **35**, 101848. doi: 10.1016/j.jobe.2020.101848
31. Y.I. Kuznetsov, Physicochemical aspects of metal corrosion inhibition in aqueous solutions, *Russ. Chem. Rev*., 2004, **73**, no. 1, 75–87. doi: 10.1070/RC2004v073n01ABEH000864
32. A. Pradityana, S. Subowo, A. Anzip, D.M.E. Soedjono, E. Widiyono and R. Prayogi, Inhibition mechanism on mango peels as organic inhibitor in 1 M HCl solution, *AIP Conference Proceedings*, 2018, **1983**, 050018. doi: 10.1063/1.5046291
33. E.F. Olasehinde, B.E. Agbaffa, M.A. Adebayo and J. Enis, Corrosion protection of mild steel in acidic medium by titanium-based nanocomposite of *Chromolaena odorata* leaf extract, *Mater. Chem. Phys*., 2022, **281**, 125856. doi: 10.1016/j.matchemphys.2022.125856
34. A. Pradityana, Sulistijono, Subowo, Suhariyanto, H. Subiyanto and L. Rusdiyana, Langmuir adsorption isotherm analysis on the addition of *Myrmecodia Pendans* extract as a corrosion inhibitor with a variety of corrosive media, *AIP Conf. Proc*., 2017, 100006. doi: 10.1063/1.4982323
35. P. Muthukrishnan, B. Jeyaprabha and P. Prakash, Adsorption and corrosion inhibiting behavior of *Lannea coromandelica* leaf extract on mild steel corrosion, *Arabian J. Chem*., 2017, **10**, S2343–S2354. doi: 10.1016/j.arabjc.2013.08.011

♦ ♦ ♦